Massive Stars Near and Far
Proceedings IAU Symposium No. 361, 2024
J. Mackey, J. S. Vink, & N. St-Louis, eds.
doi:10.1017/S1743921322002125

Spectroscopic analyses of massive stars at different metallicities

Wolf-Rainer Hamann

Institute for Physics and Astronomy, University Potsdam, D-14476 Potsdam, Germany
email: wrh@astro.physik.uni-potsdam.de

Abstract. Adequate stellar atmosphere models are prerequisite to derive robust stellar parameters from spectroscopic analyses. I will briefly review recent results obtained with the Potdam Wolf-Rayet (PoWR) model atmosphere code, which is applicable to all types of hot stars. Using multi-wavelength observations including the UV, we analyzed large samples of massive stars at various metallicities, gaining important insights on their cosmic role and the feedback to their environment.

A recent extension of PoWR allows to compose the model atmosphere from two zones. A rapidly rotating star, e.g., might possess a cooler equatorial region with a slow wind, and two polar cones with higher photospheric temperature and fast wind. For two examples of rapidly rotating O-type stars, we demonstrate that such model can reproduce wind-line profiles which otherwise would stay inconsistent. Fast rotation, which prevails in particular at low metallicities, thus might bias empirically derived parameters, having implications for feedback as well as for angular-momentum losses of SN and GRB progenitors.

Keywords. stars: atmospheres; stars: winds, outflows

1. Introduction

Detailed information on massive stars and their winds are obtained by comparing spectroscopic observations with synthetic spectra. Hot-star atmospheres and winds can be simulated with, e.g., the *Potsdam Wolf-Rayet* (PoWR) model atmosphere code. It calculates the non-LTE radiative transfer in hot-star atmospheres and winds in spherical symmetry. Complex model atoms and iron-line blanketing are taken into account. Various grids of models for Wolf-Rayet and O-type stars at different metallicities are accessible via the web interface http://www.astro.physik.uni-potsdam.de/PoWR/.

Originally focusing on Wolf-Rayet (WR) stars, the hydrogen-deficient nature of WN, WC and WO (nitrogen, carbon, and oxygen) stars was confirmed, establishing the distinction between very luminous "late-subtype" WN stars (WNL) which typically exhibit some hydrogen in their atmosphere, while the hotter "early" subtypes (WNE) are hydrogen-free (Hamann et al. 1995, 2019). A similar pattern was found in the Large Magellanic Cloud (Hainich et al. 2014), while in the Small Magellanic Cloud (SMC) *all* WN stars are hotter than the hydrogen main sequence (i.e. WNE), but at the same time are displaying hydrogen in their atmospheric composition (Hainich et al. 2015). This has been discussed as indication of strong internal mixing and quasi-homogeneous evolution under the condition of the SMC's low metallicity. Generally, the WR analyses have revealed many open issues with stellar evolution modeling, including the role of mass-loss, rotation, internal mixing, overshooting and close-binary evolution.

Applying PoWR models to O- and B-type stars, large samples at different metallicities have been studied. Figure 1 displays a Hertzsprung-Russel diagram (HRD) for massive

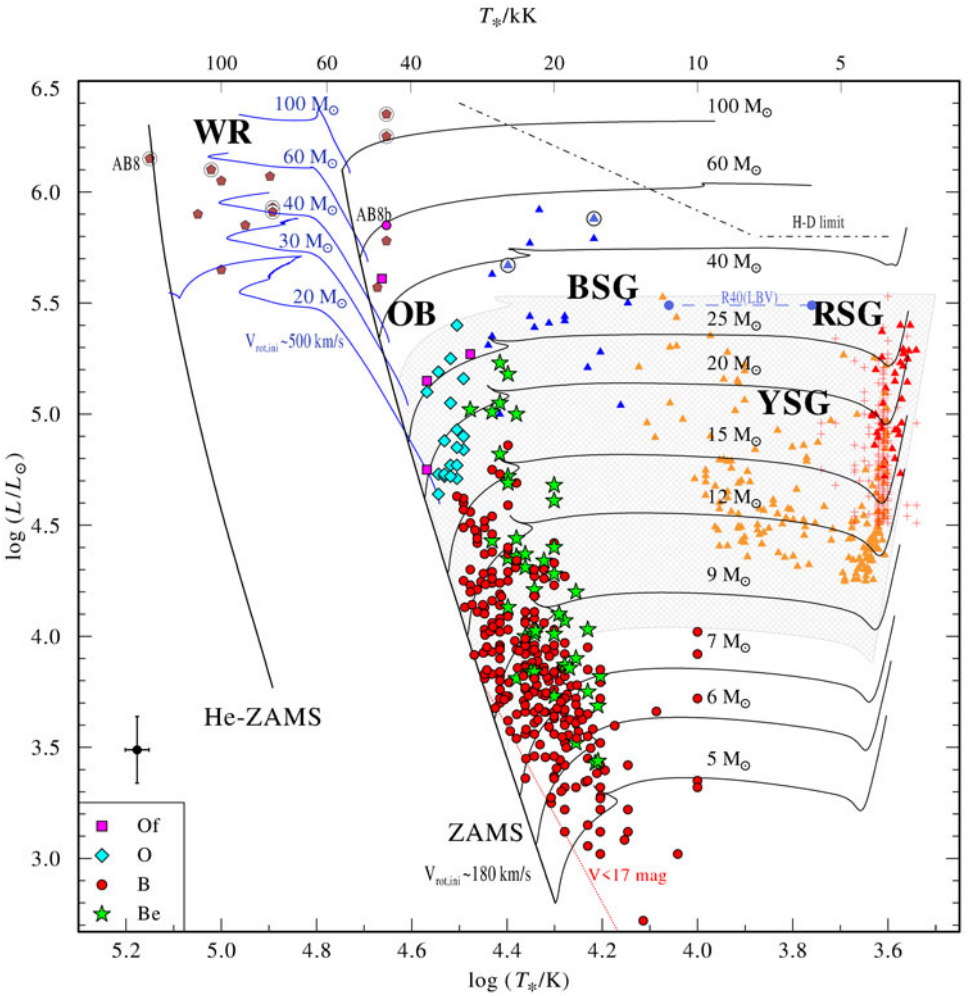

Figure 1. Hertzsprung-Russell-diagram of massive stars in the SMC (from Ramachandran et al. 2019). The OB stars analyzed in that work (symbols as specified in the inset) reside in the SMC's "Wing", while other symbols denote stars from all over the SMC (for more details see the original paper). Known binaries are encircled. Single-star evolutionary tracks shown for comparison are for modest rotation (black lines, labeled with their initial mass), while the blue lines are for very rapid rotation.

stars in the SMC (from Ramachandran et al. 2019). The most-luminous stars are located close to the hydrogen zero-age main sequence (H-ZAMS), or even to its hot side (WRs). These stars would be explainable with quasi-homogeneous evolution. The striking pattern is the sparsity, or even absence, of any other stars that would correspond to an initial mass $> 30\,M_\odot$ and non-homogeneous evolution. This dichotomy could be a consequence of rapid rotation because of reduced angular-momentum losses from weaker stellar winds due to low metallicity. If, alternatively, this pattern could just result from the SMC's particular star formation history plus observational biases remains to be shown.

2. Rotation

Stellar rotation broadens spectral lines by the Doppler effect. If a line forms in layers that are not extended, but can be approximated as the surface of a sphere, rotational

https://doi.org/10.1017/S1743921322002125 Published online by Cambridge University Press

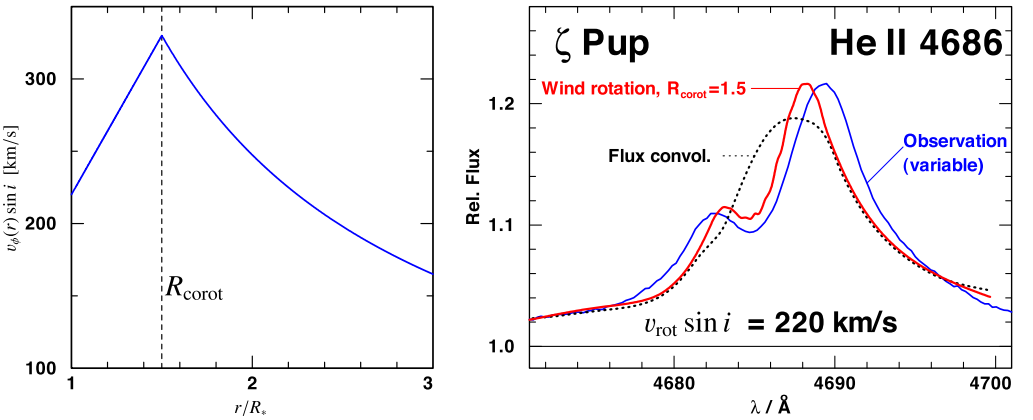

Figure 2. *Left panel:* Projected azimuthal velocity component in the equatorial plane as function of radial distance in units of the stellar radius R_*, assuming rigid-body rotation inside a co-rotation radius of $R_{\rm corot} = 1.5R_*$ and angular momentum conservation outside. *Right panel:* Profile of the He II line at 4686 Å in the spectrum of ζ Puppis; the observation (blue line) is compared to the PoWR model simulation with wind rotation (red line). The black dotted line is the synthetic profile, but rotationally broadened by convolution of the emergent flux.

broadening can be easily simulated by convolving the emergent spectrum with a semi-ellipse, or a similar function when limb darkening is taken into account. The broadening function depends only $v_{\rm rot} \sin i$, with $v_{\rm rot}$ being the rotation velocity at the equator and i the inclination angle of the rotation axis against the line of sight.

In case of spectral lines formed in a stellar wind, this approximation does not hold. In order to specify how the atmosphere follows the stellar rotation, we assume that up to some co-rotation radius $R_{\rm corot}$ the atmosphere rotates like a solid body, while outside of $R_{\rm corot}$ the azimuthal velocity component v_ϕ drops conserving angular momentum (see Fig. 2, left panel). Meridional velocity components are neglected in PoWR (Shenar et al. 2014).

The remarkable impact of such wind-rotation is demonstrated in the right panel of Fig. 2 for the He II line at 4686 Å of the prototypical supergiant ζ Pup (spectral type O4I(n)fp). The observation, albeit highly variable, mostly exhibits a double-peak profile as in this particular observation shown here.

Convolution of the emergent model spectrum with rotational broadening totally fails to reproduce the line shape. The wind rotation simulation, however, qualitatively reproduces the observed double-peak profile, if some co-rotation of the wind is assumed. One can now vary the co-rotation radius and the velocity gradient (via the β-law exponent) in order to fit in detail the (variable) observed profile. In any case, the co-rotation of the inner wind provides indirect evidence for the existence of magnetic fields that are sufficiently strong to enforce co-rotation, but must not be globally organized for not violating the upper limit from Zeeman polarization studies.

3. Non-spherical winds

In case of very fast rotation that becomes comparable with critical (break-up) rotation, stars and winds deviate from spherical symmetry. For an approximate treatment, PoWR allows to combine two different models, e.g. one for the polar cones and one for the remaining, lower latitudes. Both models are first calculated separately, thus neglecting the mutual radiative interaction between the two domains, but combined in the formal integration of the intensities emerging towards the observer.

https://doi.org/10.1017/S1743921322002125 Published online by Cambridge University Press

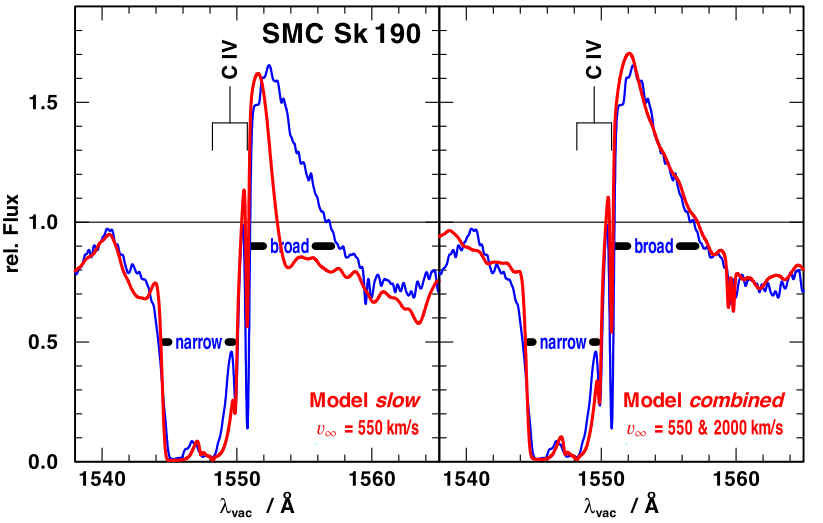

Figure 3. C IV resonance doublet in the spectrum of the SMC star Sk 190 (blue: observation). *Left panel:* The absorption feature of this P Cygni profile is narrow and fits with a PoWR model for a slow wind ($v_\infty = 550$ km/s); however, the width of the emission part of the observed profile is much broader. *Right panel:* The whole profile can be consistently reproduced by a model that combines a fast polar wind ($v_\infty = 2000$ km/s) with a slower outflow at low latitudes. The polar cone has a half opening angle of 60° and an effective temperature of 36 kK, while the model for the equatorial zone is somewhat cooler (30 kK) due to gravity darkening. A high inclination angle has been adopted ($i = 80°$).

As one example, such model is applied for simulating the C IV resonance doublet in the UV spectrum of Sk 190 in the SMC (spectral type O7.5(f)np). Photospheric lines indicate rapid rotation with $v \sin i = 300$ km/s. Figure 3 (left panel) shows the observation with HST-STIS (blue line) together with a PoWR model (red line) adopting a terminal wind velocity of $v_\infty = 400$ km/s, which is just adequate to fit the narrow absorption part of the P-Cygni profile. However, this model predicts a much narrower emission part than observed. The right panel shows the synthetic spectrum as obtained from combining a fast (∼2000 km/s) polar wind with a slow equatorial wind, now perfectly matching the whole profile. The adopted geometry is sketched in the left panel of Fig. 4. Rotational broadening is treated with wind rotation as described above.

Another obvious application of such two-zonal model is the Galactic O-type star ζ Oph. This naked-eye object has been classified as spectral type O9.5V(e)nn, where the letter "e" reflects that the star has been observed at some epochs with double-peaked emission lines as evidence for a stellar disk (Ebbets 1981). Its rotation velocity is extremely high, $v \sin i = 400$ km/s.

When fitting the C IV resonance doublet in the UV spectrum, a notorious mismatch is encountered (e.g. Marcolino et al. 2009). The observed profile exhibits a significant extra absorption in the line center at about zero Doppler shift, which cannot be reproduced with any standard wind model (pink-colored area in Fig. 5, left panel). Rotational broadening is treated with wind rotation as described above.

But when adopting an equatorial region with basically zero radial expansion velocity, this disk-like structure partially obscures part of the photosphere as seen from the observer (see the sketch in the right panel of Fig. 4), and the observed profile is roughly reproduced (Fig. 5, right panel). The sharp "narrow absorption components" observed at a Doppler blue-shift of about $-v_\infty$ are not explainable with any smooth-wind models, as has been discussed in the literature.

https://doi.org/10.1017/S1743921322002125 Published online by Cambridge University Press

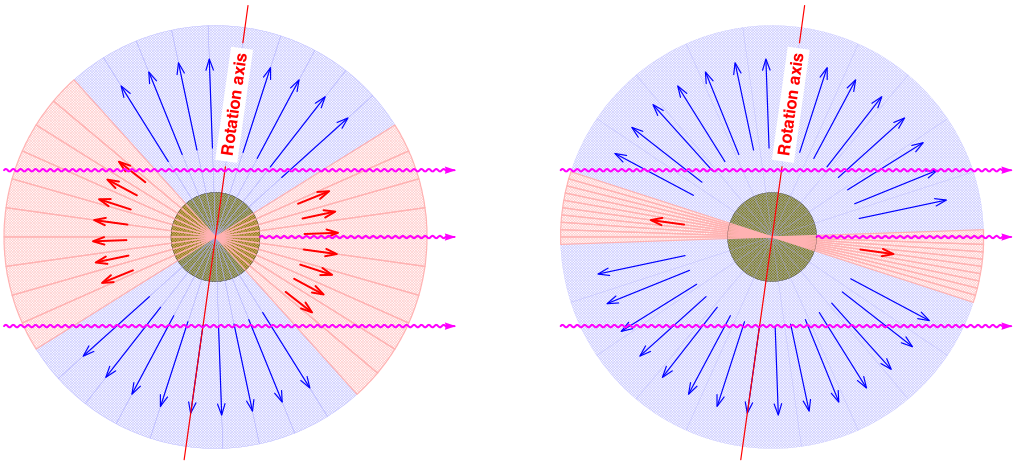

Figure 4. *Left panel:* Sketch of the geometry of the two-zone model for Sk 190. From the observer located to the right, nearly the whole stellar surface is seen through the slow wind of the equatorial zone. Therefore, the absorption part of the P-Cygni profile is narrow, according to a maximum blue-shift of $-v_\infty$. Those rays which are missing the stellar disk, however, collect emission from the fast polar wind, including matter in the back hemisphere that shows large red-shift leading to the broad emission part. *Right panel:* Sketch of the geometry of the two-zone model for ζ Oph. As seen from the observer located to the right, the disk-like region obscures roughly half of the stellar surface, causing an extra absorption at about zero Doppler shift.

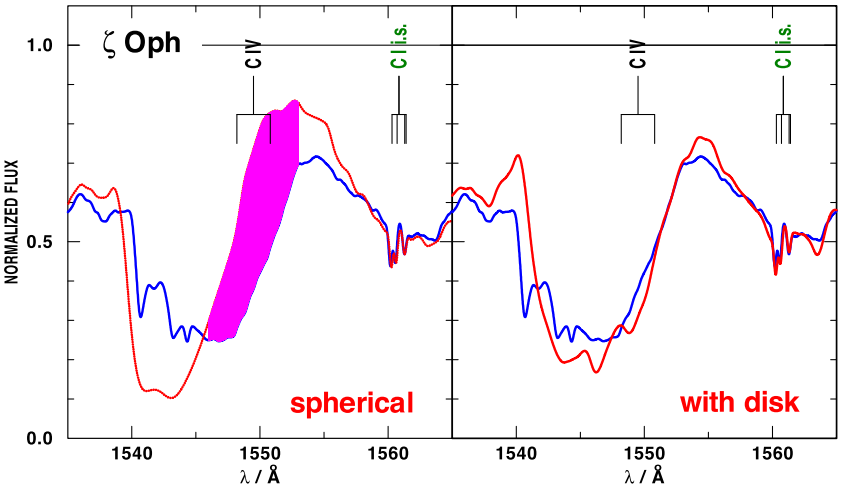

Figure 5. C IV resonance doublet in the UV spectrum of the bright Galactic O-type star ζ Oph. *Left panel:* HST-STIS observation (blue) compared to a standard (i.e. spherically symmetric) wind model ($T_* = 31.8$ kK, $v_\infty = 1600$ km/s). The observed absorption in the line center is not reproduced (pink area). *Right panel:* The central absorption is reproduced when the wind model from the left panel is combined with a disk-like equatorial region that shows no significant radial expansion. In this calculation, this disk is assumed to fill the latitudes within $\pm 5°$ and to be seen edge-on ($i = 90°$). From Henggeng Han (priv. comm.)

Apart from the excess of un-shifted absorption, ζ Oph is an example for the *weak wind problem*. The mass-loss rate, $\log \dot{M} = -9.0$ $[M_\odot/\mathrm{yr}]$ in the shown models, is by orders of magnitude lower than predicted theoretically for a radiation-driven wind from such a luminous star ($\log L/L_\odot = 4.86$) with solar metallicity – for instance, the recipe by Vink et al. (2000) yields a 50 times higher value for $\dot{M}$. In the calculation of the wind

https://doi.org/10.1017/S1743921322002125 Published online by Cambridge University Press

profiles we took already into account that the population of C IV is somewhat reduced by the (observed) X-ray field, but this does not resolve the discrepancy. The plausible explanation for the weak-wind problem has been suggested by Huenemoerder et al. (2012): the bulk of the wind plasma might be shock-heated. Thus, the true mass-loss rate can be much higher than what we detect via UV wind lines.

4. Summary

• Stellar and wind parameters of massive stars are routineously obtained by spectral analyses with adequate model atmospheres.

• Results reveal open issues with stellar evolution (mass-loss, mixing, overshooting, close-binary evolution).

• Rapidly rotating stars have non-spherical winds, with noticeable effects on their spectra which can be modeled in first approximation.

References

Ebbets, D. 1981, PASP, 93, 119
Hainich, R., Pasemann, D., Todt, H., et al. 2015, A&A, 581, A21
Hainich, R., Rühling, U., Todt, H., et al. 2014, A&A, 565, A27
Hamann, W. R., Koesterke, L., & Wessolowski, U. 1995, A&A, 299, 151
Hamann, W. R., Gräfener, G., Liermann, A., et al. 2019, A&A, 625, A57
Huenemoerder, D. P., Oskinova, L. M., Ignace, R., et al. 2012, ApJL, 756, L34
Marcolino, W. L. F., Bouret, J. C., Martins, F., et al. 2009, A&A, 498, 837
Ramachandran, V., Hamann, W. R., Oskinova, L. M., et al. 2019, A&A, 625, A104
Shenar, T., Hamann, W. R., & Todt, H. 2014, A&A, 562, A118
Vink, J. S., de Koter, A., & Lamers, H. J. G. L. M. 2000, A&A, 362, 295

https://doi.org/10.1017/S1743921322002125 Published online by Cambridge University Press